Int J Earth Sci (Geol Rundsch) (2008) 97:353–363
DOI 10.1007/s00531-007-0216-9

ORIGINAL PAPER

# Regional and local geothermal conditions in the northern Black Sea

**R. I. Kutas · J. Poort**

Received: 11 January 2007 / Accepted: 30 May 2007 / Published online: 12 July 2007


**Abstract** More than 100 new heat flow measurements have been collected in recent years (2002–2004) in different tectonic environments of the northern Black Sea. The northern periphery of the Black Sea is characterized by strong geodynamic and seismic activity, high sedimentation rates, diapiric structures, mud volcanism, and fluid and gas escape at the sea floor. We present new thermal data from the shelf, continental slope and deep-water basin, measured off-shore using a marine thermo-probe and on-shore in drill holes. Heat flow density ranges from 20 to more than 2,000 mW/m$^2$. For two local areas (the Dnieper gas seeps and the Dvurechenski mud volcano area), we discuss the relation between heat flow variability and the geological and physical processes in the near-bottom sediment layer. The Dnieper gas seeps area is characterized by strong small-scale heat flow variability and is controlled by fluid and gas migration. In the Dvurechenski active mud volcano, the near-bottom temperature in sediments is anomalously elevated because additional heat is carried out by mass flows of fluids and clay minerals. Away from the mud volcano heat flow quickly decreases to background values.

R. I. Kutas (✉)
Institute of Geophysics,
National Academy of Ukraine,
32 Palladin Ave, 03680 Kiev 142, Ukraine
e-mail: kutro@ndc.org.ua

J. Poort
Renard Centre of Marine Geology (RCMG),
Universiteit Gent, Krijglaan 281 s8,
9000 Gent, Belgium

**Keywords** Black Sea · Temperature · Heat flow · Gas seeps · Mud volcano

## Introduction

A rather large number of geothermal measurements have been carried out in the northern Black Sea basin. The results suggest that low heat flow density prevail in the studied region. In the central deepest parts of the basin, heat flow does not exceed 20–40 mW/m$^2$ (Duchkov and Kazantsev 1985, 1988; Erickson and von Herzen 1978; Golmshtok and Zolotarev 1980; Kobolev et al. 1993; Kobzar 1987; Konduirin and Sochelnikov 1983; Kutas et al. 1998, 1999, 2002, 2005; Lubimova and Savostin 1973; Zolotarev et al. 1979). At the periphery, on the shelf and on the Andrusov Ridge, heat flow density is considerably higher. The range of its variation also widens from 15–20 to100–150 mW/m$^2$. Considering these wide variations of heat flow, the available data have not been sufficient to come to firm conclusions on the intensity, extent, and especially, on the nature of the anomalies.

This article presents heat flow density data collected in northern part of the Black Sea in 2002–2004 within two projects, the Ukrainian project "Mineral resources of the Ukraine" and the EC 5th framework project "Crimea", carried out on the research vessel Professor Vodyanitski (cruises 57–61). The study areas include the northern part of the deep-sea basin, continental slope and outer margin of the shelf. They are both morphologically and geologically very complex and not yet completely understood. On the shelf, the heat flow has been measured in boreholes, whereas in deep-water basin it was measured with the conventional marine thermo-probe method. The sea water depth in the area varies from 100 to 2,150 m.

## Geological setting

The Black Sea is a marginal basin with a water depth of 2–2.2 km. It is part of the Alpine folded belt, which consists of various young structural units, including the Pontides-Balkanides to the south–southwest, the Caucasus to the east, the Crimea Mountains to the north and the Moesian and Scythian platform to the west and northwest. These orogenic belts form the marginal part of the basin, shelf and continental slope of the Black Sea (Fig. 1) (Tugolesov et al. 1985; Finetti et al. 1988; Robinson et al. 1996; Nikishin et al. 2003). The Black Sea depression formed during the Late Cretaceous in a back-arc setting.

At the level of the crystalline basement, the Black Sea consists of two basins, the Western and the Eastern Black Sea basins, separated by the Mid-Black Sea or Andrusov ridge. They are filled with Meso-Cenozoic sediments with a total thickness of 16–18 km in the Western Black Sea basin and 12–14 km in the Eastern basin. In the central part of the basin, the sedimentary cover is characterized by sub-horizontal stratification, whereas its offshore parts contain asymmetric folds and thrusts.

The under-laying basaltic crust of the deep basins does not exceed 5–15 km in thickness (Tugolesov et al. 1985; Finetti et al. 1988). On the basin periphery, however, the continental crustal thickness reaches up to 40–50 km and Cenozoic stratigraphic complexes become thinner or completely disappear. Tectonically, the Black Sea periphery is composed of various features of different origin and age, such as tectonic ridges (Andrusov, Shatski, Arhangelski and others) and troughs of marginal basin type related to Cretaceous (Karkinit) or Late-Cenozoic (Sorokin, Tuapse) orogenic activity.

Intensive present-day tectonic activity, seismicity, mud volcano activity, gas and fluid escapes are concentrated in the northern part of the Black Sea (Kutas et al. 2002, 2004). Here we present thermal details of two areas where gas seepage and mud volcanism prevails: the Dnieper paleo-delta and the Dvurechenski deep-sea area. The Dnieper paleo-delta is situated in the NW part of the Black Sea on the continental slope, at water depths of 250–840 m, between the West Crimea Fault and the Odessa Fault. It is featured by a complex system of canyon-fan type and ridges. The main canyon system is the Dnieper canyon in the eastern part of study area. A large number of gas seeps were detected on echo sounding records during the Crimea expeditions (Naudts et al. 2006). The Dvurechenski study area is situated in the deep basin of the Black Sea in the Sorokin trough along the southeastern margin of the Crimean Peninsula, at water depths of 1,900–2,100 m. The trough began to form in the Oligocene and it has now an infill of 9 km of mid-Late Cenozoic deposits: over 5 km of argillaceous Maikopian deposits (Oligocene to low Miocene) and 3.5–4 km of Middle Miocene-Quaternary deposits (Tugolesov et al. 1985; Limonov et al. 1994). A multiple phases compressional tectonic regime from Oligocen to Quaternary (Nikishin et al. 2003) folded the Maikopian sediments and overlying deposits and intruded them with diapirism. This created favorable pathways for mud, fluid and gas escape.

## Method and equipment

Marine geothermal data were collected using the GEOS-2 (Matveev and Rot 1988) thermo-probe, suitable for deep-water basins. The GEOS measuring system consists of a submerging thermo-probe, connected to an on-board unit by a three-core cable-rope. The marine thermo-probe is composed of a pressure case containing the electronics and fixed to the top of a lance to which two separate full-length (2.5 m) out rigged probes are attached. One probe is used for temperature and thermal gradient measurements and consists of five temperature elements equally spaced at half meter intervals, whereas the other probe is used for the in-situ thermal conductivity measurements and contains a linear heat element in combination with four copper sensors. The configuration of the probe allows to obtain both thermal gradient and thermal conductivity over the same depth interval. The temperature at the

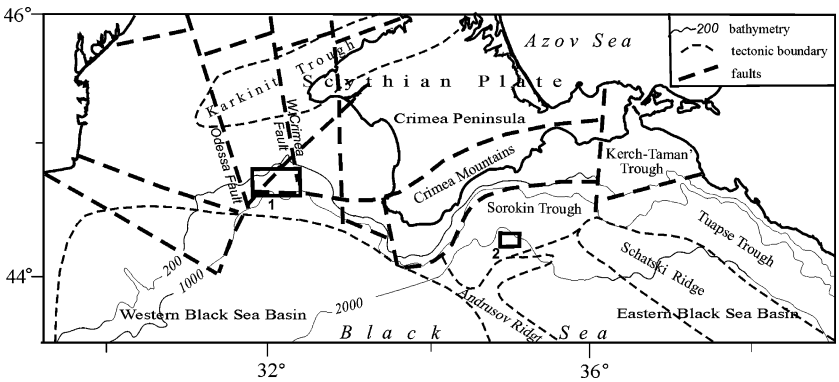


**Fig. 1** Map of the northern Black Sea with indication of the major tectonic elements and location study areas of detailed thermal investigations (*rectangles*): *1* the Dnieper paleo-delta and *2* the Dvurechenski area)

bottom sensors is measured absolutely to an accuracy of 0.005 K, while temperatures at the other four sensors are measured relative to the bottom sensor. Measuring errors on geothermal gradient and thermal conductivity are approximately 5%. Tilting of the probe is recorded with an accuracy of 5°.

The penetration depth of the sensors is estimated by means of (1) the recorded temperature rise during probe insertion, (2) the difference in temperature curves resulting from heating in water and sediments during thermal conductivity measurements, and (3) the interval temperature gradients. The uncertainty of the sensor's absolute position is not more than the distance between two sensors and between the upper sensor and the container (both 0.5 m).

Once the frictional heating fades away, the thermal conductivity of sediments is measured in-situ with an independent heating experiment using continuous line-source method (von Herzen and Maxwell 1959). Heat flow density is computed for each depth interval as the product of the thermal gradient and thermal conductivity, and then it is averaged.

Real-time monitoring during probe lowering allows to control the instrument performance and data quality. After penetration into the sediments, the probe is left undisturbed for 10–15 min; the conductivity measurement starts about 4–5 min later. All geothermal data are logged at 4 s intervals. The sensors thermal inertia is approximately 12–15 s.

An example of a full temperature record of in-situ thermo-probe measurement is shown in Fig. 2. Three parts of the temperature record deliver specific information on the thermal state and physical properties of sea floor sediment. The first part relates to temperature data of the near-bottom water and of the frictional heating events during probe insertion. The second part includes the temperature data in the sediments to compute the interval thermal gradients. The last part characterizes the thermal properties of the deposits and how the local environment reacts to temperature increase resulting from the heat release during the thermal conductivity measurement. Information from each of the three parts of the record is important for the estimation of the geothermal parameters or physical conditions near the measurement site.

Frictional heating during probe insertion raises the temperature of the probe and the surrounding sediment. The amplitude of this thermal pulse depends on sediment properties and on the time-length of insertion of each sensor. Deeper sensors are heated to higher temperatures than shallow ones. The cooling history of the frictional heat decay can be used for the determination of the thermal conductivity and the equilibrium temperature (Lee and von Herzen 1994; Lee et al. 2003). In an ideal case, conformity between thermal gradients and thermal conductivity should

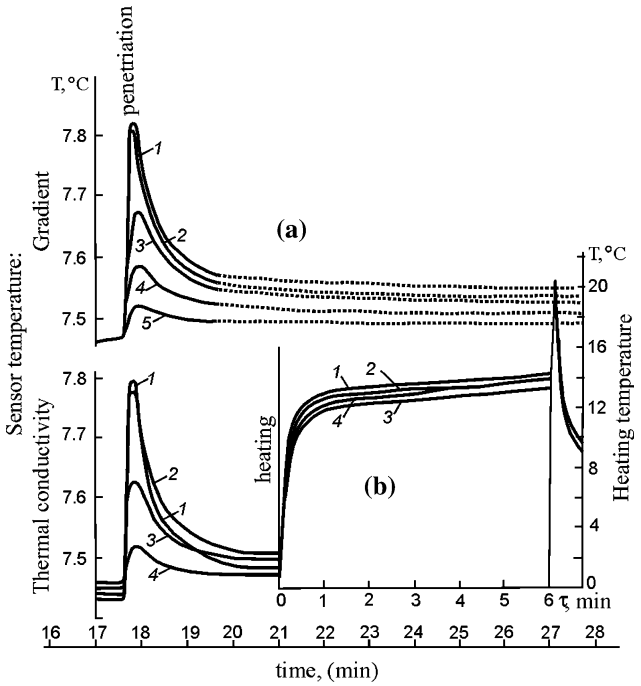


**Fig. 2** Example of a typical temperature record of Geos-2 thermo-probe in-situ measurement: **a** sub-bottom temperatures measured at the 5 different sensors, showing the penetration heating of the probe and the consequent cooling to equilibrium and **b** the insertion frictional heating and the controlled constant heating curves which are used to calculate the thermal conductivity. The spike at the end of the heating curve is connected with frictional heating during probe pull out

be established in equilibrium conditions. The absence of such conformity testifies to the existence of disturbing processes. The probe insertion may form a thin zone of disturbed sediment around the probe and may cause pore fluids to flow.

## Results

New heat flow measurements were performed at 108 stations: seven stations are deep boreholes on the shelf, all other measurements have been carried out by the thermo-probe method in the upper meters of soft sediments of the continental slope and the deep-water basin, during several cruises.

The borehole thermal data on the northwestern shelf are from boreholes located in Karkinit trough. Heat flow determinations were made at sub-bottom depths from 1,200 to 2,800 m and interested Miocene, Oligocene and Eocene terrigenous and carbonate deposits. The final results of the borehole geothermal data are listed in Table 1. The heat flow density ranges from 50 to 75 mW/m$^2$, with lower values found in the deep part of the Karkinit trough and enhanced values on the trough flanks. The thermal conductivity varies

**Table 1** Results of definition of heat flow density in deep boreholes

| $N_0$ | Boreholes | Coordinates | | Gradients, K/m | Thermal conductivity W/m K | Heat flow, mW/m$^2$ |
|---|---|---|---|---|---|---|
| | | N | E | | | |
| 1 | Golitsyna-4 | 45°43′ | 31°53′ | 0.040 | 1.85 | 74 ± 8 |
| 2 | Golitsyna-2 | 45°40′ | 31°58′ | 0.035 | 1.95 | 65 ± 6 |
| 3 | Shtormovaya-5 | 45°15′ | 31°40′ | 0.037 | 1.80 | 66 ± 8 |
| 4 | Shtormovaya -2 | 45°15′ | 31°42′ | 0.040 | 1.80 | 72 ± 8 |
| 5 | Gamburtseva-2 | 45°13′ | 31°22′ | 0.025 | 2.00 | 50 ± 5 |
| 6 | Selskogo-40 | 45°08′ | 31°33′ | 0.037 | 1.90 | 70 ± 10 |
| 7 | Olympic -400 | 44°45′ | 30°32′ | 0.033 | 1.75 | 57 ± 8 |

between 1.4 and 1.8 W/m K for argillaceous sediments and between 1.6 and 2.2 W/m K for carbonates.

Offshore thermo-probe measurements are made at water depths larger than 300 m because at shallower depths seasonal bottom water temperature variations are too large (Kutas et al. 1999; Poort et al. 2007). Sea bottom temperature in the Black Sea changes from 8.66 ± 0.03°C at 300 m water depth to 9.1 ± 0.1°C at 2,200 m water depth. Thermo-probe thermal measurements have been collected in the Western Black Sea basin-deep, in the Eastern basin-deep, on the Andrusov ridge, in the Sorokin trough, and on continental slope. Results of these measurements are listed in Table 2.

Low heat flow density (20–35 mW/m$^2$) have been obtained in the Western Black Sea basin, where the greatest thickness of sediments occur. Higher heat flow values have been measured in the Eastern Black Sea basin (ranging from 27 to 57 mW/m$^2$) and on the Andrusov ridge (43–54 mW/m$^2$). The strongest heat flow variations are revealed on the basin periphery. On the whole area of the continental slope heat flow changes from 20 to 87 mW/m$^2$. Maxima are obtained on active mud volcanoes and over diapiric structures, where heat flow sometimes increases up to hundreds and even to thousands mW/m$^2$.

Temperature-depth profiles in most stations are near-linear, but deviations are observed in many areas, characterized by both low and high thermal gradients (Fig. 3).

Deviations from linearity are in general not a result of an anomalous thermal conductivity structure of the sediment (thermal refraction). Measured in-situ sediment thermal conductivities vary from 0.65 to 1.6 W/m K, but the majority falls in the range of 0.75–1.10 W/m K with a normal compaction-related increase with depth for most stations. Some stations, however, recorded anomalous thermal conductivity distributions and values such as: (1) a thermal conductivity decrease with depth, (2) abnormal sharp changes with depth, and (3) extremely large values of 3–4 W/m K, in a station with hydrate-containing sediments. These anomalous thermal conductivity stations are all located within zones of mud volcanism, intensive gas and/or water dynamics.

Two areas on the periphery with strong heat flow variability have been investigated in more detail: the Dnieper paleo-delta on the continental slope and the Dvurechenski mud volcano area in the Sorokin trough (Fig. 1). On the Dnieper paleo-delta area, the heat flow measurements were made in water depth of 300–840 m in 24 stations (Fig. 4).

These data are listed in Table 2 and have also been incorporated in Poort et al. (2007). The majority of the thermal stations are located on the top and the flanks of the sloping ridge structure where seepage is widely spread. Several heat flow stations were made in the Dnieper canyon. On the Dnieper paleo-delta area sea bottom temperature increases from 8.66°C at 300 m depth to 8.85°C at 850 m depth. At 2.5 m sub-bottom depth temperature changes from 8.74 to 9.15°C. Thermal gradient ranges from 20 to 80 mK/m and averages to 41 mK/m. Heat flow ranges from 22 to 87 mW/m$^2$, with an average value of 37 ± 10 mW/m$^2$. Increased heat flow 40–54 mW/m$^2$ appears to be related to active tectonic structures and to the West Crimea fault system. In seeps low heat flow values (22–28 mW/m$^2$) with consistent "Z-type" vertical gradient curves were observed: the thermal gradient decreases in the lower part of the measured interval and increases in its middle or upper part. The gradient decrease is often accompanied by a thermal conductivity decrease.

In the Dvurechenski area geothermal parameters were measured in 24 stations, 9 of which are located in the Dvurechenski mud volcano crater, 14 around the mud volcano, and 1 in the new Vodyanitski mud volcano (Table 2).

Both in and around the mud volcanoes anomalous variations in the geothermal parameters have been identified. In the Dvurechenski at 2.5 m sub bottom depth the temperature changes from 9.1 to 20.17 °C (Fig. 5). The high temperatures form two anomalies in central northwestern and in southeastern parts of the volcano. These high sediment temperatures, as compared to the constant ambient bottom temperatures of 9 ± 0.1°C, suggest upward advective transport of deep, warmer material.

**Table 2** Results of definition of heat flow density in Black Sea

| $N_0$ | $N_0$ stations | Coordinates | | Depth, m | Gradients, K/m | Thermal conductivity, W/m K | Heat flow, $mW/m^2$ |
|---|---|---|---|---|---|---|---|
| | | N | E | | | | |
| **Cruise 57 (2002)** | | | | | | | |
| 1 | 5615 | 44°14.7′ | 34°47.2′ | 2020 | 0.053 | 1.14 | 60 ± 4 |
| 2 | 5616 | 44°16.8′ | 34°54.1′ | 2038 | 0.070 | 1.08 | 75 ± 6 |
| 3 | 5616г | 44°19.8′ | 35°01.7′ | 2035 | 0.035 | 1.25 | 44 ± 7 |
| 4 | 5617 | 44°23.0′ | 35°09.0′ | 1818 | 0.038 | 1.22 | 46 ± 9 |
| 5 | 5618 | 44°25.9′ | 35°19.5′ | 1755 | 0.038 | 1.12 | 42 ± 10 |
| 6 | 5622▲ | 44°16.9′ | 34°58.8′ | | 0.036 | 1.36 | 50 ± 10 |
| 7 | 5624 | 44°14.4′ | 34°46.9′ | 2113 | 0.036 | 1.21 | 43 ± 6 |
| 8 | 5625 | 44°19.9′ | 34°50.0′ | 2052 | 0.040 | 1.31 | 52 ± 10 |
| 9 | 5626 | 44°23.7′ | 34°53.0′ | 2015 | 0.043 | 1.41 | 56 ± 5 |
| 10 | 5627 | 44°28.0′ | 34°57.0′ | 1900 | 0.044 | 1.33 | 59 ± 11 |
| 11 | 5628 | 44°37.0′ | 35°03.5′ | 1445 | 0.064 | 1.30 | 62 ± 7 |
| 12 | 5648 | 44°28.0′ | 34°19.8′ | 500 | 0.029 | 1.30 | 38 ± 4 |
| 13 | 5649 | 44°22.6′ | 34°19.6′ | 640 | 0.030 | 1.15 | 34 ± 5 |
| 14 | 5650 | 44°15.9′ | 34°20.1′ | 1050 | 0.044 | 1.32 | 59 ± 9 |
| 15 | 5651 | 44°16.6′ | 34°29.9′ | 2000 | 0.042 | 1.15 | 48 ± 12 |
| 16 | 5653 | 44°29.1′ | 34°31.5′ | 1500 | 0.058 | 1.08 | 54 ± 8 |
| 17 | 5660■ | 44°17.0′ | 34°58.0′ | 2047 | 0.068 | 1.37 | 93 ± 16 |
| 18 | 5661▲ | 44°17.1′ | 34°58.9′ | 2055 | 0.305 | 1.22 | 372 ± 26 |
| 19 | 5663 | 44°15.3′ | 35°20.8′ | 1984 | 0.048 | 1.29 | 62 ± 10 |
| 20 | 5664 | 44°15.05′ | 34°20.06′ | 1993 | 0.056 | 1.29 | 60 ± 6 |
| 21 | 5664A | 44°15.0′ | 35°35.0′ | 1821 | 0.055 | 1.44 | 80 ± 12 |
| 22 | 5665 | 44°15.0′ | 35°50.0′ | 1766 | 0.036 | 1.26 | 45 ± 7 |
| 23 | 5666 | 44°15.1′ | 36°05.2′ | 1722 | 0.024 | 1.25 | 30 ± 8 |
| 24 | 5667 | 44°10.1′ | 36°15.1′ | 1790 | 0.044 | 1.31 | 58 ± 9 |
| 25 | 5668 | 44°00.1′ | 36°14.9′ | 2041 | 0.029 | 1.22 | 35 ± 6 |
| 26 | 5669 | 43°45.1′ | 36°15.3′ | 2037 | 0.033 | 1.27 | 42 ± 9 |
| 27 | 5670 | 43°29.8′ | 36°20.1′ | 2022 | 0.033 | 0.94 | 31 ± 10 |
| 28 | 5671 | 43°34.7′ | 35°55.7′ | 2193 | 0.037 | 1.17 | 43 ± 11 |
| 29 | 5672 | 43°42.2′ | 35°30.4′ | 2200 | 0.038 | 1.15 | 44 ± 16 |
| 30 | 5673 | 43°49.5′ | 35°06.8′ | 2204 | 0.037 | 1.21 | 45 ± 5 |
| 31 | 5674 | 43°56.9′ | 34°40.9′ | 2195 | 0.036 | 1.25 | 43 ± 6 |
| 32 | 5675 | 44°03.8′ | 34°13.9′ | 2084 | 0.049 | 1.12 | 54 ± 10 |
| 33 | 5676 | 44°11.0′ | 34°04.9′ | 826 | 0.034 | 1.10 | 37 ± 4 |
| 34 | 5678 | 44°05.0′ | 35°36.8′ | 1603 | 0.100 | 1.28 | 128 ± 17 |
| 35 | 5679 | 44°11.8′ | 35°19.7′ | 1874 | 0.064 | 1.17 | 80 ± 14 |
| 36 | 5682 | 44°20′ | 32°46.9′ | 1722 | 0.025 | 1.09 | 27 ± 4 |
| 37 | 5683 | 44°17′ | 32°47′ | 743 | 0.035 | 1.11 | 39 ± 11 |
| 38 | 5684 | 44°16.6′ | 32°51.3′ | 1772 | 0.033 | 1.12 | 37 ± 12 |
| 39 | 5685 | 44°17′ | 32°55.9′ | 804 | 0.034 | 1.12 | 40 ± 10 |
| 40 | 5688 | 43°08.2′ | 37°35.5′ | 2163 | 0.042 | 1.36 | 47 ± 14 |
| 41 | 5689 | 42°53′ | 38°25.5′ | 2126 | 0.040 | 1.37 | 56 ± 8 |
| **Cruise 58 (2003)** | | | | | | | |
| 1 | HF1* | 44°39.15′ | 32°08.95′ | 822 | 0.030 | 0.855 | 32 ± 4 |
| 2 | HF2* | 44°42.05′ | 32°05.72′ | 646 | 0.020 | 1.009 | 22 ± 8 |
| 3 | HF3* | 44°43.29′ | 32°04.42′ | 577 | 0.031 | 0.930 | 28 ± 6 |
| 4 | HF4* | 44°42.84′ | 32°02.85′ | 646 | 0.020 | 1.309 | 26 ± 7 |

**Table 2** continued

| $N_0$ | $N_0$ stations | Coordinates | | Depth, m | Gradients, K/m | Thermal conductivity, W/m K | Heat flow, $mW/m^2$ |
|---|---|---|---|---|---|---|---|
| | | N | E | | | | |
| 5 | HF5* | 44°44.02′ | 32°05.79′ | 545 | 0.026 | 0.920 | 24 ± 6 |
| 6 | HF7* | 44°46.58′ | 31°58.11′ | 306 | 0.068 | 0.913 | 62 ± 9 |
| 7 | HF9* | 44°46.53′ | 31°59.72′ | 265 | 0.025 | 1.113 | 28 ± 3 |
| 8 | HF10* | 44°46.45′ | 31°54.85′ | 324 | 0.054 | 0.730 | 40 ± 4 |
| 9 | HF11* | 44°50.65′ | 32°11.95′ | 500 | 0.062 | 0.880 | 54 ± 4 |
| 10 | HF12* | 44°50.79′ | 32°11.59′ | 480 | 0.053 | 0.851 | 49 ± 6 |
| 11 | HF13* | 44°49.25′ | 32°13.95′ | 600 | 0.074 | 0.668 | 50 ± 3 |
| 12 | HF14* | 44°50.01′ | 32°10.02′ | 371 | 0.054 | 0.822 | 45 ± 8 |
| 13 | HF15■ | 44°16.90′ | 34°58.76′ | 2074 | 0.032 | 1.029 | 33 ± 7 |
| 14 | HF16▲ | 44°16.70′ | 34°59.12′ | 2086 | 0.142 | 1.022 | 140 ± 29 |
| 15 | HF17■ | 44°17.95′ | 35°00.49′ | 2117 | 0.063 | 1.129 | 71 ± 9 |
| 16 | HF18■ | 44°16.14′ | 35°02.53′ | 2125 | 0.040 | 0.937 | 38 ± 6 |
| 17 | HF19 | 44°43.48′ | 36°00.83′ | 395 | 0.030 | 0.897 | 27 ± 7 |
| 18 | HF20 | 44°17.46′ | 34°59.73′ | 2102 | 0.042 | 1.113 | 52 ± 10 |
| 19 | HF21□ | 44°17.72′ | 35°02.10′ | 2070 | 0.259 | 0.949 | 244 ± 9 |
| 20 | HF22■ | 44°17.74′ | 35°01.43′ | 2081 | 0.047 | 1.012 | 50 ± 3 |
| 21 | HF23■ | 44°18.45′ | 34°58.71′ | 2070 | 0.040 | 0.958 | 38 ± 5 |
| 22 | HF26■ | 44°17.38′ | 34°59.64′ | 2097 | 0.067 | 0.852 | 59 ± 6 |
| 23 | HF27▲ | 44°16.69′ | 34°59.10′ | 2084 | 0.305 | 3.320 | 310 ± 37 |
| **Cruise 59 (2003)** | | | | | | | |
| 1 | 5750 | 44°04.37′ | 33°37.02′ | 1650 | 0.060 | 1.043 | 63 ± 16 |
| 2 | 5755 | 43°55.06′ | 33°35.91′ | 2024 | 0.058 | 0.945 | 54 ± 9 |
| 3 | 5756 | 43°49.06′ | 33°44.83′ | 2097 | 0.042 | 0.953 | 40 ± 7 |
| 4 | 5761 | 44°25.22′ | 35°15.66′ | 1742 | 0.042 | 1.000 | 42 ± 4 |
| 5 | 5762▲ | 44°16.82′ | 34°58.83′ | 2074 | 0.083 | 1.045 | 83 ± 13 |
| 6 | 5763▲ | 44°17.24′ | 34°59.53′ | 2095 | 0.056 | 1.090 | 61 ± 4 |
| 7 | 5764 | 44°18.58′ | 34°59.34′ | 2070 | 0.049 | 0.871 | 42 ± 6 |
| 8 | 5765 | 44°17.03′ | 34°57.15′ | 2122 | 0.068 | 1.113 | 75 ± 7 |
| 9 | 5769▲ | 44°17.01′ | 34°58.88′ | 2093 | 0.233 | 1.010 | 240 ± 21 |
| **Cruise 60 (2004)** | | | | | | | |
| 1 | HF28* | 44°44.30′ | 32°05.25′ | 527 | 0.035 | 0.862 | 30 ± 9 |
| 2 | HF29* | 44°44.92′ | 32°04.35′ | 475 | 0.038 | 0.810 | 31 ± 7 |
| 3 | HF30* | 44°42.80′ | 32°04.10′ | 605 | 0.045 | 0.823 | 37 ± 6 |
| 4 | HF31* | 44°42.12′ | 32°03.82′ | 735 | 0.062 | 0.850 | 48 ± 5 |
| 5 | HF32* | 44°42.27′ | 32°03.77′ | 730 | 0.035 | 0.905 | 31 ± 5 |
| 6 | HF33* | 44°42.13′ | 32°03.90′ | 735 | 0.049 | 0.896 | 45 ± 9 |
| 7 | HF34* | 44°42.94′ | 32°06.01′ | 655 | 0.042 | 0.870 | 37 ± 9 |
| 8 | HF35* | 44°42.43′ | 32°06.82′ | 675 | 0.031 | 0.885 | 37 ± 8 |
| 9 | HF36* | 44°41.75′ | 32°08.29′ | 728 | 0.043 | 0.858 | 36 ± 3 |
| 10 | HF37* | 44°40.86′ | 32°03.80′ | 852 | 0.041 | 0.810 | 31 ± 7 |
| 11 | HF38* | 44°42.75′ | 32°05.15′ | 647 | 0.028 | 0.960 | 27 ± 3 |
| 12 | HF39* | 44°41.05′ | 32°05.98′ | 725 | 0.094 | 0.929 | 87 ± 9 |
| 13 | HF40■ | 44°17.97′ | 35°01.20′ | 2056 | 0.047 | 1.150 | 54 ± 6 |
| 14 | HF41■ | 44°17.58′ | 35°01.66′ | 2076 | 0.053 | 1.197 | 62 ± 9 |
| 15 | HF43■ | 44°17.30′ | 35°02.57′ | 2080 | 0.053 | 1.297 | 66 ± 10 |
| 16 | HF44■ | 44°18.15′ | 34°58.74′ | 2058 | 0.040 | 0.890 | 35 ± 3 |

**Table 2** continued

| $N_0$ | $N_0$ stations | Coordinates | | Depth, m | Gradients, K/m | Thermal conductivity, W/m K | Heat flow, $mW/m^2$ |
|---|---|---|---|---|---|---|---|
| | | N | E | | | | |
| **Cruise 61 (2005)** | | | | | | | |
| 1 | 5780▲ | 44°17.01′ | 34°58.80′ | 2068 | 2.720 | – | ~2500 ± 520 |
| 2 | 5781 | 44°15.60′ | 35°00.40′ | 2122 | 0.039 | 1.020 | 40 ± 4 |
| 3 | 5782 | 44°15.51′ | 34°58.65′ | 2133 | 0.050 | 0.966 | 51 ± 3 |
| 4 | 5783 | 44°37.80′ | 36°01.17′ | 665 | 0.022 | 0.880 | 20 ± 3 |
| 5 | 5784 | 44°40.98′ | 36°00.88′ | 636 | 0.024 | 0.905 | 22 ± 4 |
| 6 | 5785 | 44°38.17′ | 36°03.58′ | 688 | 0.024 | 0.880 | 21 ± 6 |
| 7 | 5786 | 44°35.89′ | 36°00.95′ | 837 | 0.028 | 0.868 | 24 ± 2 |
| 8 | 5788■ | 44°17.70′ | 35°00.40′ | 2052 | 0.049 | 0.905 | 44 ± 4 |
| 9 | 5789▲ | 44°17.24′ | 34°59.26′ | 2053 | 0.062 | 0.952 | 60 ± 14 |
| 10 | 5791 | 43°33.97′ | 31°38.07′ | 1866 | 0.026 | 0.903 | 23 ± 3 |
| 11 | 5796 | 44°33.80′ | 31°43.99′ | 817 | 0.037 | 0.970 | 36 ± 6 |

* Dnieper gas seeps area

▲ Dvurechenski mud volcano

■ Surrounding Dvurechenski mud volcano area

□ Vodyanitski mud volcano

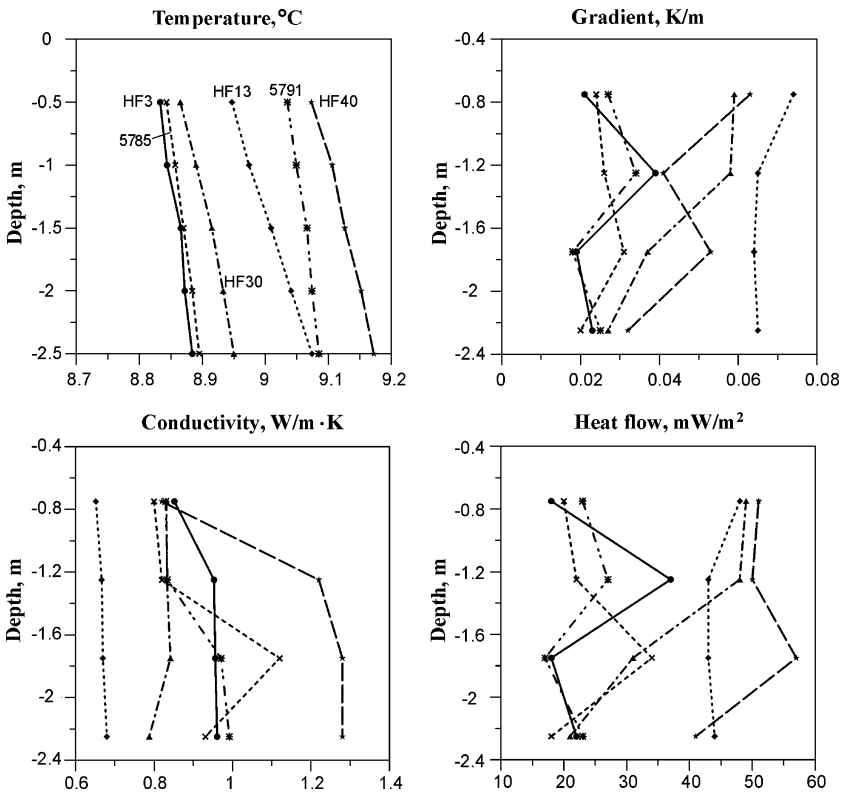


**Fig. 3** Vertical variability of thermal parameters (temperature, geothermal gradient, thermal conductivity) for six stations in the northern Black Sea illustrating near-linear temperature-depth profiles and a normal compaction-related increase of thermal conductivity with depth observed in most stations. Deviations of this pattern are observed in different areas and discussed in the main text. Station numbers are marked on the temperature curves

## Discussion

In different areas of the Black Sea the thermal field in the near-bottom sediments is locally strongly disturbed. Notable variations of geothermal parameters are seen on the continental slope, in fault zones, in areas of gas and fluid dynamics, mud volcanism, and in gas and gas hydrate saturated deposits. The local character of the heat flow variations exclude regional factors such as deep structural and thermophysical heterogeneities, and points to small

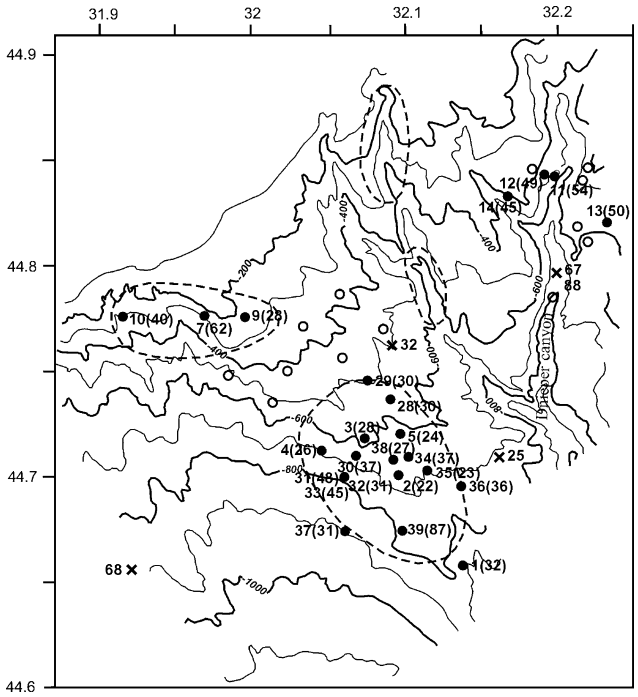


**Fig. 4** Bathymetry and new (*black dots*) and existing (*crosses*) heat flow data in the Dnieper study area (station number with heat flow values in *parenthesis*). *Open circles* are separated gas seeps, the *dashed lines* show areas of dense clusters of gas escape

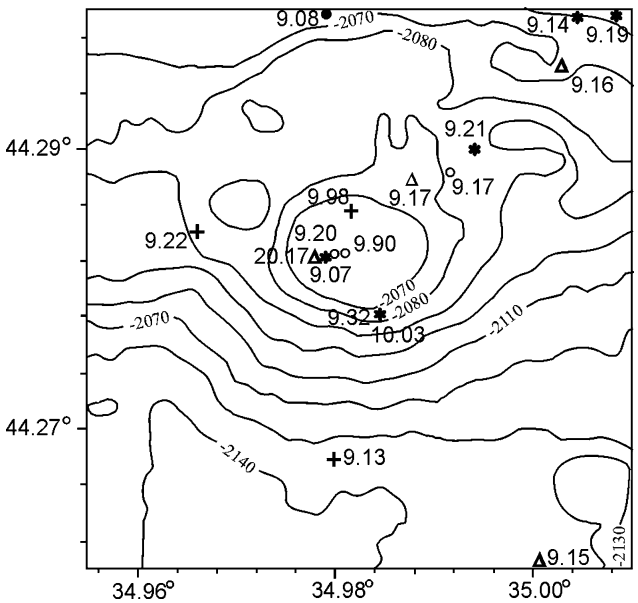


**Fig. 5** Temperature measurements (in °C) at the sub-bottom depth of 2.5 m in the Dvurechenski mud volcano area in 2002–2004: cruise 57 (*crosses*), 58 (*stars*), 59 (*open circles*), 60 (*black circles*) and 61 (*triangles*)

near-bottom disturbances that may result from seafloor morphology, bottom water temperature changes, fluid advection and heat sources or sinks in the sediment. The sea floor sediments undoubtedly host many different physical and chemical processes that are characterized by heat release or absorption and that affects the heat transfer mechanism. Also the thermo-probe insertion into the sediment and the heating during conductivity measurement may influence the measurement results, as it can result in changes of physical properties of the surrounding sediments. In depth analysis of the temperature record from the in-situ temperature and thermal conductivity measurements reveals important information about the nature of the geothermal parameters. Below we discuss several records illustrating both typical and anomalous thermal stations.

Figure 6 shows three temperature records during the course of probe insertion into sediments that display particular features for three different sites. The first temperature record (Fig. 6a) is from station 5791, located in the Western Black Sea depression on a flat bottom surface and with absence of fluid or gas transport features. The frictional heating and cooling history of thermo-probe shows the typical (ideal) pattern, identical to the record in Fig. 2. They display a synchronous cooling of all sensors that reach (in approximately 1.5–2 min) in-situ temperature that differs no more than 10–15% from equilibrium. Average temperature gradient is 26 ± 4 mK/m and the thermal conductivity increases with depth from 0.83 to 0.99 W/m K. Heat flow density varies from 17 to 27 mW/m$^2$, with an average value of 23 ± 3 mW/m$^2$ (Fig. 3). Similar geothermal features prevail in all deep-water part of the Black Sea. Other areas, however, often display anomalous records. For example, in the station HF 13 (Fig. 6b), located in the Western Crimea fault zone, the insertion is not well expressed by the temperature increase and the cooling of frictional heating occurs very slowly. The temperature gradient decreases with depth from 74 to 64 mK/m and the thermal conductivity falls to 0.65–0.68 W/m·K (Fig. 3). Such geothermal conditions can be explained as the result of a weak outflow of warm water and an accumulation of free gas around thermo-probe after insertion. This type of record has been registered mainly at the bottom of the continental slope, on mud volcanoes and on isolated gas seeps. Another example is station HF 30 (Fig. 6c), located in the Dnieper paleo-delta, in an area of intense gas emission. Here the frictional heating during insertion is higher for the shallower sensors than for the deeper ones. The temperature gradient decreases from 52 mK/m in the upper part to 36 mK/m in the bottom part (Fig. 3). Such anomalous feature can be explained by the presence of a gas pocket very close to the surface (Poort et al. 2007). Probe penetration through the sealing crust and into the gas pocket will result in gas ebullition (by fracturing of the seal) and pressure release in the gas pocket. This provides the necessary pathway for free gas to escape and for cold water to infiltrate. In this case, equilibrium temperatures

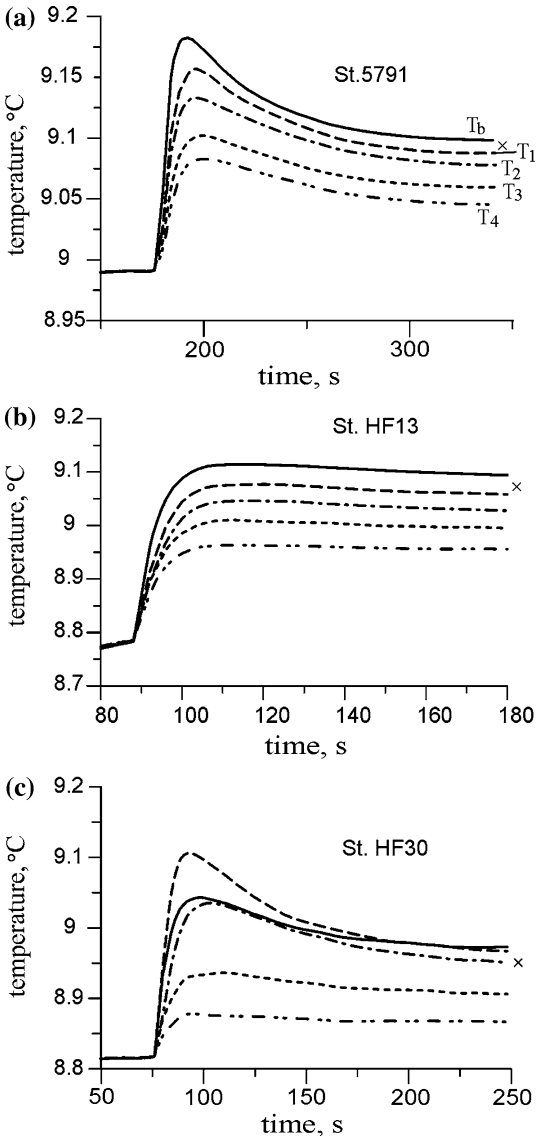


**Fig. 6** Temperature records of thermo-probe insertion into sediment in three different sites illustrating the influence of fluid and gas transport processes: **a** a normal record from the western Black Sea depression, **b** warm up flow of fluids along the West Crimea fault and **c** cold water infiltration in Dnieper paleo-delta area. For more explanation: see text. *1–5* are numbers of probe sensors from deep to shallow. *Crosses* represent equilibrium temperatures of the bottom sensors

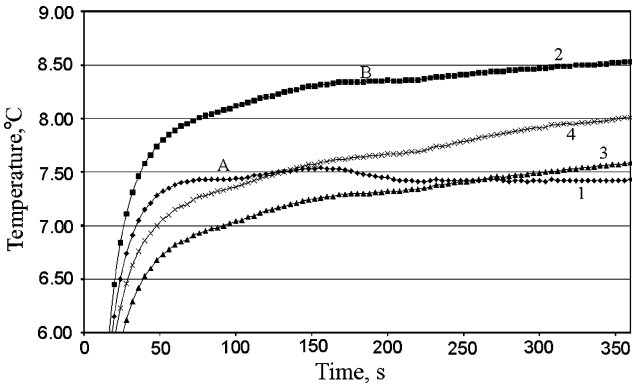


**Fig. 7** Heating curves for the thermal conductivity determination in station 5796 where gas hydrate inclusion have been recovered. *Curves* at two of the four sensors show anomalous behavior: **a** Disturbed part of the temperature curve 50 s after start of heating recorded by bottom sensor; **b** similar heating temperature disturbance after 200 s since heating start, recorded by second deeper sensor. Numeration of sensors is from deep to shallow

are only established after long time. Similar temperature records have been observed in other areas of intensive gas release.

An example of an anomalous in-situ thermal conductivity record is shown in Fig. 7. Using the continuous line source method, the determination of thermal conductivity is achieved on the basis of the amount of heat sent into the sediments. Therefore, any processes that absorb heat (flow of cold water, decomposition of gas hydrates and other), will reduce the rate of heating near the probe and result in an over-estimation of the thermal conductivity. On the contrary, processes increasing the temperature around the probe (flow of warm water or gas) will result in lowered "apparent" values of thermal conductivity. Figure 7 shows the thermal conductivity record of station 5796, located on the basin slope at water depth of 820 m, and illustrates the effect of gas hydrate containing sediments on a thermal conductivity measurement. The presence of gas hydrates in the form of separate crystals in this site was confirmed by direct sampling. At this station the geothermal gradients shows normal values ranging from 35 mK/m for the top interval to 25 mK/m for the bottom interval (Fig. 8). The thermal conductivity, on the other hand, displays an anomalous behavior. For several intervals an apparent thermal conductivity is calculated of up to more than 4 W/m K (Fig. 8). In the thermal conductivity record (Fig. 7) it can be seen how heating after 40–50 s raised the temperature of the bottom sensor by 7.4°C relative to the sediment temperature prior to heating (8.96°C) and reached a temperature of approximately 16.5°C. From that time on the temperature increase stopped although heating continued. We believe that this anomalous pattern can be best explained by the decomposition of the observed gas hydrate inclusions around the thermo-probe. For the water depth of station 5796 the temperature of phase equilibrium for methane hydrates is approximately 12°C (Berecz and Balla-Achs 1983; Sloan 1990). During the thermal conductivity measurement in this station a temperature of more than 12°C is reached up to approximately 1 mm away from the probe of the bottom sensor. For the second sensor the temperature record suggests the presence of hydrate inclusions, at 2.5 mm away from the sensor (equals to 200 s after the beginning of constant heating). Repeated

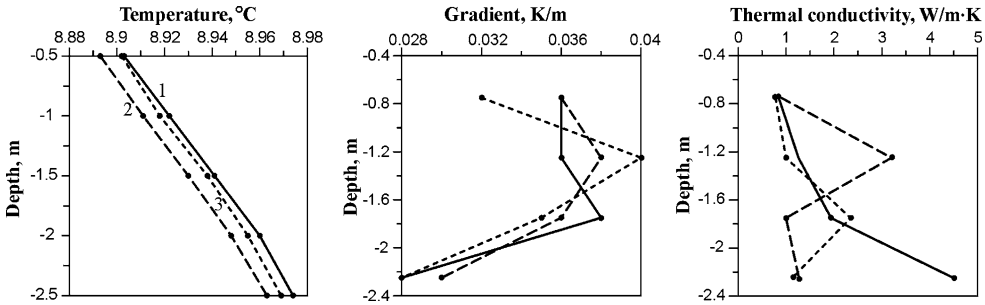


**Fig. 8** The vertical variability of thermal parameters at station 5796 shows the anomalous large "apparent" thermal conductivities at several sensors (see also Fig. 7), while temperatures and geothermal gradients are within the expected range

thermo-probe measurements in station 5796 all show the same distortion while temperature gradients remain consistent to normal values.

The analysis of different geothermal parameters indicate that the measured enhanced and reduced heat flow values in the northern Black Sea are in most cases the result of mass movement of pore waters or muds. For positive anomalies heat is brought up by fluids and argillaceous substance from deeper levels, while reduced heat flow can result from infiltration of cold sea water. These reduced heat flow anomalies are found near the top of ridges, in seep system and in mud volcanoes. The driving force for these infiltrations may be related to the presence of large gas concentrations. The gas phase in sediments occurs either as a dissolved component, as a free gas, or as gas hydrate. When the thermodynamic conditions change, the gas equilibrium can be disturbed, producing gas escape. This process provides the necessary pressure change for water flow and thus is indirectly responsible for the observed changes of thermal parameters.

## Conclusion

New geothermal studies made in the northern Black Sea evidence the existence of local heat flow anomalies superimposed on top of a regular regional distribution, related to the Cenozoic tectonic and sedimentary history. The local heat flow anomalies are due to disturbed conditions of heat transfer in an over pressurized sedimentary environment. Analysis of the heat flow distribution in relation to the locations of fluid-and-gas outlets, mud volcanoes and diapir structures, suggests that focused fluid flow results from pore waters and gas being discharged near the flanks of the Black Sea basin.

**Acknowledgement** The authors are very grateful to reviewers Dr. V. Cermak (Geophysical Institute of the Academy of Sciences of the Czech Republic), Dr. B. Della Vedova (Universita di Trieste, Italy), Dr. A.Duchkov (Institute of Geophysics Russian Academy of Sciences Siberian Branch) for their comments and recommendation.). We are indebted to Jan Klerkx, Oleg Kravchuk, Michail Bevzyuk, Jeroen Vercruysse, Lieven Naudts and Marc De Batist, with the help of whom we collected the thermal data. J. Poort is supported by a post-doctoral research assistantship of the Flemish Fund for Scientific Research (FWO-Vlaanderen).

## References

Berecz E, Balla-Achs M (1983) Gas hydrates. Acad Kiado, Budapest, pp 1–343

Duchkov AD, Kazantsev CA (1985) Heat flow through bottom of the Black Sea (in Russian). Geol Geofiz 8:113–123

Duchkov AD, Kazantsev CA (1988) Heat flow of the Black Sea depression. In: Geophysical fields of the Atlantic Ocean (in Russian). Nauka, Moscow, pp 121–130

Erickson AJ, von Herzen RP (1978) Downhole temperature measurements and heat flow data in the Black Sea. Int Rep DSDP leg 426 Washington 42(2):1085–1103

Finetti GD, Bricchi G, Del Ben A, Pipan M, Xuan Z (1988) Geophysical study of the Black Sea. Boll Geofis Teor Appl XXX 117–118:197–324

Golmshtok AJ, Zolotarev VG (1980) Deep-seated heat flow of the Black Sea Basin (in Russian). Dokl Akad Nauk SSSR 254:956–959

Kobolev VP, Kutas RI, Tsvyashchenko VA (1993) Geothermal studies in the northern part of the Black Sea (in Russian). Geofiz Zh 15:61–72

Kobzar VM (1987) Heat flow and block structure of the lithosphere of the Black Sea depression (in Russian). Geofiz Zh 8:90–94

Kondiurin AB, Sochelnikov VV (1983) Geothermal flow in western part of the Black Sea (in Russian). Okeanologiya 23:622–627

Kutas RI, Kobolev VP, Tsvyashchenko VA (1998) Heat flow and geothermal model of the Black Sea depression. Tectonophysics 291:91–100

Kutas RI, Kobolev VP, Tsvyashchenko VA, Bevzjuk MI, Kravchuk OP (1999) Results of heat flow determination in the northwestern Black Sea (in Russian). Geofiz Zh 21:38–51

Kutas RI, Rusakov OM, Kobolev VP (2002) Gas seeps in the northwestern Black Sea: geological and geophysical studies. Russian Geol Geophys 43:698–705

Kutas RI, Paliy SI, Rusakov OM (2004). Deep faults, heat flow and gas leakage in the northern Black Sea. Geo-Marine Lett 24:163–168

Kutas R, Poort J, Klerkx J, Kravchuk O, Bevzyuk M (2005) Geothermal conditions in zones of gas escape and mud volcanism in northern Black Sea. Geophys J 27:128–135

Lee TC, von Herzen RP (1994) In-situ determination of thermal properties in sediments using friction-generated probe source. J Geophys Res 99:12121–12132

Lee TC, Duchkov AD, Morozov SG (2003) Determination of thermal conductivity and formation temperature from cooling history of friction heated probes. Geophys J Intern 152:433–442

Limonov AF, Woodside JM, Ivanov MK (1994) Mud volcanism in the Mediterranean and Black Seas and shallow structure of the Eratosthenes Seamount. UNESCO Rep Mar Sci 64:1–173

Lubimova EA, Savostin LA (1973) Heat flow in the Central and Eastern Black Sea (In Russian). Dokl Akad Nauk SSSR 212:349–352

Matveev VG, Rot AA (1988) Now development of the equipment for automation of sea geothermal researches on a shelf (in Russian). In: Geothermal investigations at the bottom of water areas. Nauka, Moscow, pp 98–107

Naudts L, Greinert J, Artemov Yu, Staelens P, Poort J, Van Rensbergen P, De Batist M (2006) Geological and morphological setting of 2778 methane seeps in the Dniepr paleo-delta, northwestern Black Sea. Marine Geology 227:177–199

Nikishin AM, Korotaev MV, Erchov AV, Bruten M–F (2003) The Black Sea basin: tectonic history and Neogene-Quaternary rapid subsidence modeling. Sediment Geol 156:149–168

Poort J, Kutas RI, Klerkx J, Beaubien SE, Lombardi S, Dimitrov L, Vassilev A and Naudts L (2007) Strong heat flow variability in an active shallow gas environment, Paleo-Dniepr, Black Sea. Geo-Mar Lett. doi:10.1007/s00367-007-0072-4

Robinson AG, Rudat JH, Banks CJ, Wills RLF (1996) Petroleum geology of the Black Sea. Mar Pet Geol 13:195–223

Sloan ED (1990) Clastrate hydrates of natural gases. Marcel Dekker, New York, pp 3–64

Tugolesov TA, Gorshkov AS, Meisner LB, Soloviev VV, Khakhalev EM (1985) Tectonics of the Meso-Cenozoic deposits of the Black Sea depression (in Russian). Nedra, Moscow, pp 3–214

Von Herzen RP, Maxwell AE (1959) The measurement of thermal conductivity of deep sea sediments by needle probe method. J Geophys Res 64:1557–1563

Zolotarev VG, Sochelnikov VV, Malovitski YuP (1979) Results of heat flow measurements in Black Sea and Mediterranean Basins. Okeanologiya 19:1059–1065